

MICROMECHANICAL ASPECTS OF CONSTRAINT EFFECTS IN STEEL FOR CONTAINERS OF SPENT NUCLEAR FUEL

I. Dlouhý, Z. Chlup

Institute of Physics of Materials, Academy of Sciences of the Czech Republic,
• i•kova 22, 616 62 Brno, Czech Republic

ABSTRACT

Arising from two-parameter fracture mechanics approach to the analysis of failure initiation condition the three point bend specimens with shallow and deep cracks were tested at various temperatures. Low carbon manganese cast steel was used for the analysis. This steel is tested as one of several candidate materials for containers of spent nuclear fuel. The effect of crack length on the fracture toughness-temperature diagram has been analysed. Although a strong dependence of measured fracture toughness on crack tip constraint was observed no evident differences in fracture morphology have been identified except for quantitative ones. Peculiarities of fracture behaviour in the transition and lower shelf regions of the steel investigated have been explained. The effect of crack tip constraint on brittle fracture characteristics has been quantified by means of the Q-parameter. The role of critical (cleavage) fracture stress in brittle fracture initiation under the influence of crack tip constraint has been analysed. A toughness scaling model applied in work has been discussed. Based on knowledge obtained the master curve methodology has been applied to predict steel fracture behaviour by using pre-cracked Charpy type specimen.

INTRODUCTION

The knowledge in assessment methods of fracture mechanics has increased to a point where certain structural materials, until now not considered for radioactive transport and storage casks design, are being proposed for these applications [1]. For the safe enclosure of the radioactive material during transportation it must be proved that the extension of non-detected cracks after fabrication will not occur even in case of most severe accident loading. For safe storage additional embrittling effects should be taken into account. Brittle fracture can occur under specific combination of temperature, mechanical and environmental loading conditions [2,3]. When assessing if the material satisfies the demand on container resistance against catastrophic failure the following key problems have to be addressed from the fracture mechanical point of view: (i) the transferability of fracture toughness data measured on laboratory specimens to the component of much larger thickness; (ii) the prediction of the probability of brittle fracture in case of the most severe accident loading and in case of radiation embrittlement.

ŠKODA Nuclear Machinery Ltd. has introduced new design of a container for spent nuclear fuel. The cask design is based on thick-walled cask with bolted lids, both fabricated from cast low alloyed steel with ferritic microstructure. Several approaches might be applied or developed in order to solve the problem of the container integrity from the point of view of material fracture resistance and its prediction including the local approach [4-6], toughness scaling models [7,8 etc.] and master curve methodology [9-12]. The capability to predict the fracture behaviour for any configuration of defect and component could be accepted as a very hard criterion of the assessment procedure.

The aim of the present contribution is to characterise the fracture resistance of cast ferritic steel predetermined for radwaste casks applying two-parameter fracture mechanics approach. Applicability of the master curve methodology has also been addressed.

MATERIAL AND EXPERIMENTAL PROCEDURES

Material characterisation

Manganese cast steel has been used having the following chemical composition in wt %: 0.09C, 1.18Mn, 0.37Si, 0.01P, 0.025S, 0.12Cr, 0.29Ni, 0.29Cu, 0.03Mo, 0.028Al. The material has been supplied in form of 270 mm thick plate produced commonly with model cask. Special heat treatment based on intercritical austenitisation was developed in order to produce homogeneous properties throughout the plate thickness.

True stress-strain curves have been determined using cylindrical specimens with a diameter of 6 mm in the temperature range -196°C to -60°C at a cross-head speed of $2\text{ mm}\cdot\text{min}^{-1}$.

The cast steel examined exhibits relatively low values of lower and upper yield stress and with decreasing temperature these characteristics increase very slowly (e.g. at -100°C the yield stress is equal to only 380 MPa). With respect to small pre-cracked specimens this fact resulted in the necessity to test small specimens at very low temperatures in order to fulfil the criteria for the determination of valid K_{Jc} values.

Mechanical testing and calculations

Fracture toughness was determined using three test specimen geometries. The first one was the standard three-point bend (1T) specimen $25\times 50\times 220\text{ mm}^3$. The other ones were selected to receive in specimen shallow cracks (a/W of about 0.2 and 0.1) and, at the same time, comparable ligament area under the crack tip. In these two specimen types the crack was introduced under condition close to standard one, then the specimens were cut and ground to final dimensions of $25\times 30\times 130\text{ mm}^3$ ($a/W \approx 0.2$) and $25\times 27\times 120\text{ mm}^3$ ($a/W \approx 0.1$). All specimens were tested at 1mm/min cross-head speed in the temperature range from -198 to -20°C . Fracture toughness values for $a/W \approx 0.5$ have been determined according to ASTM E813-89 and similar standards. For calculation of stress intensity factor for shallow cracks the general equation from handbook was applied [16]. Small pre-cracked Charpy type specimens (PCVN) have been tested statically and by low blow method in a wide temperature range. Charpy type specimens in static three point bending have also been tested in order to receive data for local approach applications. The dynamic tests (impact and low blow method) using an instrumented impact tester have also been carried out in order to follow the influence of strain rate.

The standard FEM code ABAQUS 5.7 was used to model elastic-plastic behaviour (almost in 3D) for all test specimen geometries investigated.

Extensive fractographic observations were carried out, the work is continuing and more detailed analyses will be published later.

RESULTS AND DISCUSSION

Fracture toughness and crack length effect

The temperature dependence of fracture toughness determined on specimens with standard crack length ($a/W \sim 0.5$) is shown in **Figure 1**. Two sets of specimens were tested at two selected temperatures and the data obtained are also shown in Fig. 1. The first one (-100°C) has been selected as test temperature in the lower shelf region common for all crack lengths tested supposing the same - cleavage - fracture initiation mechanism is acting in the specimens. The other temperature has been selected very close to the upper shelf region (-70°C) but still having cleavage initiation mechanism on fracture surfaces.

Only some specimens met the condition of LEFM for standard K_{Ic} toughness values and the K_{Jc} values have been obtained in almost cases. In the transition and near the upper shelf region the fracture behaviour has been characterised by K_{Jc} values determined for specimen without detectable ductile tearing before fracture and by K_{Ju} values for specimens with ductile crack extension preceding unstable fracture. Curves representing the limit (i) between the validity of LEFM and EPFM and (ii) between the constraint dependent and independent K_{Jc} values are shown in the figure. The $K_{Jc}(Q)$ values thus represent the K_J fracture

toughness in the constraint dependent regime. K_{Ji} represents the value for specimen with 0.2 mm ductile crack extension and temperature t_{DBL} the lowest temperature for the occurrence of this initiation micromechanism.

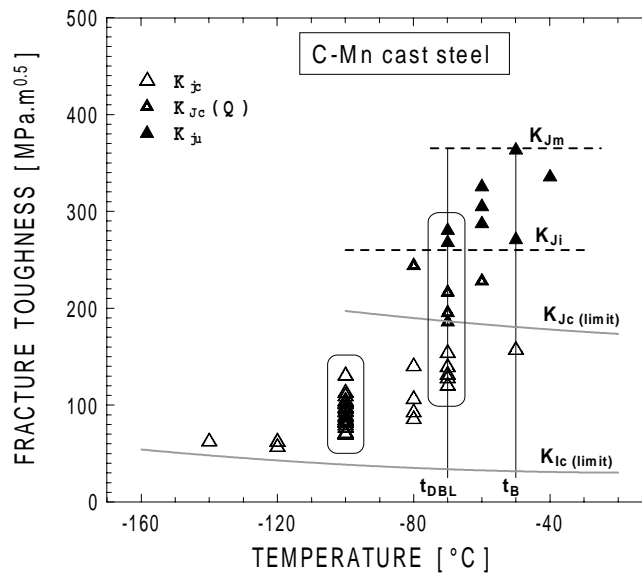


Figure 1: Fracture toughness - temperature diagram for standard specimens

Similar fracture toughness - temperature dependencies for bend specimens with shallow cracks ($a/W \sim 0.2$ and $a/W \sim 0.1$) have been obtained including the larger sets of data generated at -100 °C (common to all specimen geometries) and at the other selected temperature (at -80 and -85 °C , respectively). Exponential curves have been fitted through all three specimen configurations and sets of fracture toughness data (K_{Jc}) in transition and lower shelf region. These fits are introduced in **Figure 2**. It can be seen from this figure that very similar fracture behaviour as in the case of standard crack length (full curve) can be identified in the transition region of specimens with shallow cracks, and only quantitative differences in fracture characteristics could be observed.

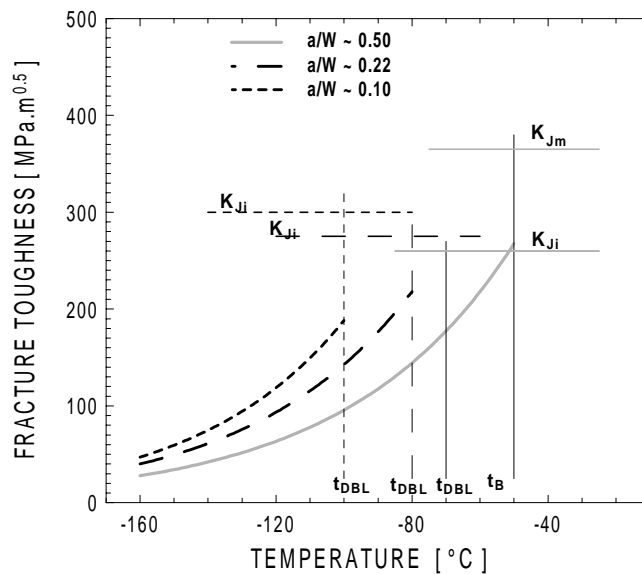


Figure 2: Crack length effect on fracture toughness data (K_{Jc}) in the transition region

The distribution of principal tensile stresses was calculated (3D) for all specimen geometries tested at -100 °C and all fracture loads measured. An attempt has been made to estimate the local cleavage fracture stress for all specimen geometries tested. This stress was calculated at the distance of the fracture initiation point as

obtained from quantitative fractographic analyses. Average values of about 1255 MPa have been estimated for specimens having standard crack length. Similarly, the local cleavage fracture stress of about 1340 MPa was obtained for specimens having $a/W \approx 0.2$.

From comparison of the main trends in fracture toughness temperature dependencies and from the FEM calculation finished until now the following important characteristics of crack length effect (and corresponding crack tip constraint effect) were found:

- A shift of the transition region (the transition temperature t_B) to lower temperatures can be observed for shallower cracks (lower constraint).
- The mean fracture toughness obtained at one test temperature (the same initiation mechanism was proved by SEM for all specimens) is comparably higher for shorter cracks when compared with standard crack length.
- A larger scatter in fracture toughness values can be observed for shorter cracks being strongly influenced by larger crack tip plastic zone (smoother maximum on principal tensile stress distributions below crack tip).
- With decreasing crack length the fracture load and the dimensions of the highly stressed region below the crack tip increase and, in addition, the principal stress corresponding to this region is higher.
- With decreasing crack length the cleavage fracture stress appears to be slightly increased, probably due to larger plastic deformation preceding the fracture initiation.

Using the experimental data obtained on specimen sets tested at -100°C , the dependence of fracture toughness on crack length was obtained as shown in **Figure 3**.

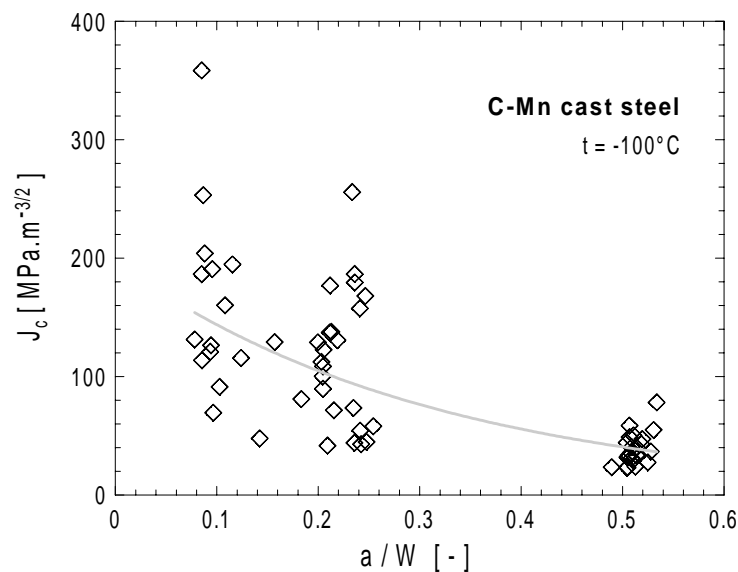


Figure 3: Crack length effect on fracture toughness

Modified approach to Q-parameter determination

In addition to the above-mentioned peculiarities (the slight increase of cleavage fracture stress for shallow cracks in particular) the steel fracture behaviour characterised by high scatter of inherent material properties and extent of plastic deformation preceding the fracture. For the same value of critical load quite different values of J_c integral have been determined due to this feature. In order to overcome the problems two approaches for the Q-parameter determination have been tested: (i) standard calculation arising from the basic definition and fracture loads measured for particular specimens and (ii) modified procedure based on more realistic critical parameter of loading - the J integral value.

Selected curves used for the determination of Q-parameter for particular specimen crack length are shown as example in **Figure 4**. For specimen geometry with shallow cracks (having a/W around 0.1) and given crack length (figures at curves) the Q-parameter was read directly from the J values corresponding to critical loads. Comparison of both approaches is shown in **Figure 5** for the crack length $a/W \sim 0.1$. The cross points

represent the values of Q-parameter determined by standard calculation, the rhombi represent the modified approach. Quite good agreement has been found, further analyses are necessary, however. By incorporating a much higher number of experimental data the statistical aspect will be necessary to be taken into account before making final conclusions.

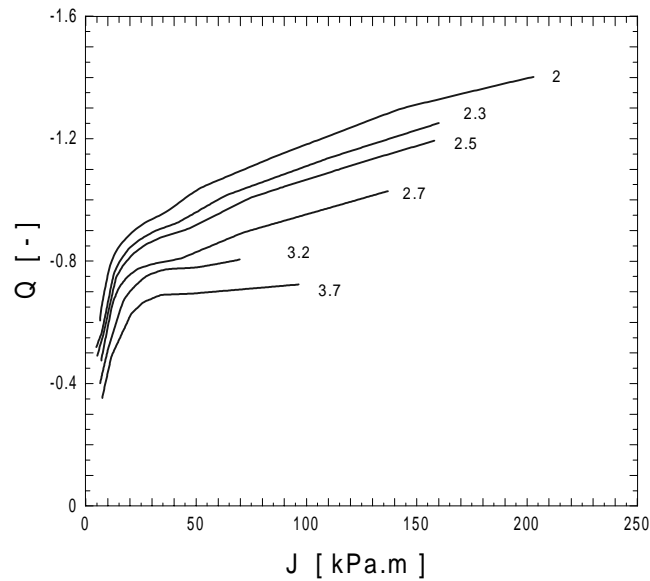


Figure 4: Diagrams used for determination of Q parameter from J-integral

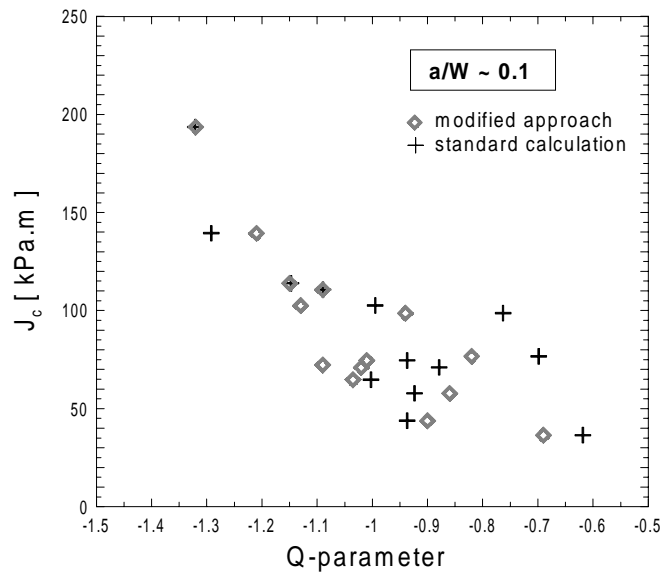


Figure 5: J-Q relation for specimen with shallow cracks and both calculation procedures

Master curve for standard 1T bend specimens.

Based on the fracture toughness obtained from tests on 23 specimens tested at the temperature of $-100\text{ }^{\circ}\text{C}$ the reference temperature T_0 was determined. All the K_{Jc} results obtained have been checked whether the basic assumption included in ASTM Standard E1921 [9] for determining the reference temperature T_0 was met, i.e. whether the cast steel tested obeys the three parametric Weibull distribution with the Weibull modulus m equal to 4. According to the procedure given in the standard the reference temperature was determined to be $T_0 = -82\text{ }^{\circ}\text{C}$ [13]. The master curve for the C-Mn cast steel studied is can thus be described by the equation:

$$K_{Jc(\text{med})} = 30 + 70 \exp[0.019(T + 82)] \quad (1)$$

In **Figure 6** the master curve together with the tolerance bounds 5% and 95% is shown. In this diagram the

fracture toughness values in the temperature range -100 to -40 °C are plotted. The full points represent data not meeting the validity condition:

$$K_{Jc(LIMIT)} = [(Eb Re) / 50]^{1/2} \quad (2)$$

The value of constant in Eq. 2 was taken to be 50 instead of 30 in the standard [9] based on work of Ruggieri et al [7] and discussion in ASTM Subcommittee E 08.08.

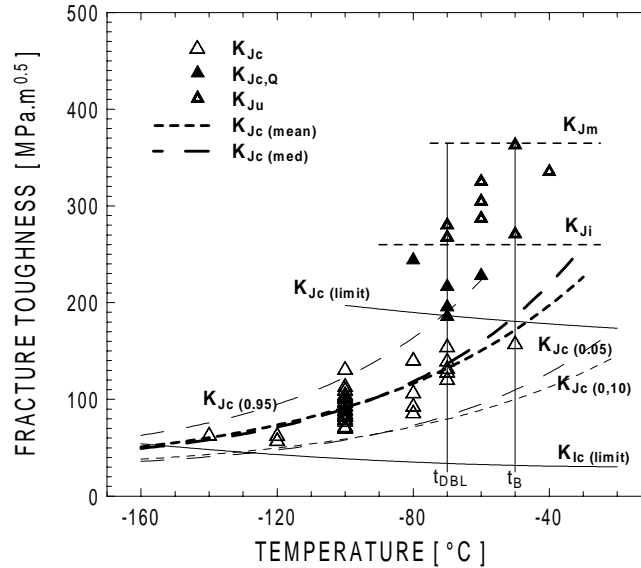


Figure 6: Master curve for 1T specimen (with data corrected on constraint)

Data lying above the limit curve, Eq. (2), represent failures in the constraint dependent regime ($Q \neq 0$). Corrections have to be introduced for these data, e.g. as proposed by Dodd and Anderson [13,14]. All the values introduced correspond well to 0.05 and 0.95 % probability band and the master curve ($K_{Jc (med)}$) obtained corresponds well to the exponential fit ($K_{Jc (mean)}$) through the experimental and constraint corrected data. Based on these analyses the master curve methodology may be successfully applied for fracture toughness assessment of the steel investigated.

Some peculiarities in fracture behaviour of cast steel follow from Figure 6 however:

- The master curve methodology may be applied to predict the fracture toughness behaviour only for the fracture toughness values being below $T_0 + 15$ °C.
- The sharp transition of fracture toughness to much higher values of K_{Jc} occurs at the temperature $T_0 + 26$ °C. But it must be emphasised that for those specimens having these high values of K_{Jc} , fracture was initiated by cleavage thus indicating that the C-Mn cast steel has large intrinsic resistance to ductile tearing.

The use of PCVN specimen for fracture toughness prediction.

Pre-cracked Charpy type specimens (PCVN) are most suitable for the assessment of radiation and thermal ageing of container cask steel as well as for analysis of strain rate effect. For PCVN specimens the temperature dependence of fracture toughness is given in **Figure 7**. The line representing the validity condition (Eq. (2)) is plotted in the graph. A relatively small number of fracture toughness data, especially the data at the temperature -100°C, that were intended for establishing T_0 , fall below this line. Therefore data not meeting the $K_{Jc}(\text{limit})$ have been constraint adjusted applying the toughness scaling model of Dodds and Anderson [14,15]. But only for data lying below the line labelled $K_{Jc}(\text{max})DA$ this concept may be used, as this line represents the end of the FE-3D calculation of Dodds and Anderson model.

By combining the toughness scaling model [14,15] and the master curve methodology the fracture toughness temperature diagram for 1T specimens can be predicted using data obtained from the pre-cracked Charpy

type specimens. All data from the PCVN specimens being adjusted for constraint effect have been additionally size corrected by using

$$K_{Jc(1T)} = 20 + (K_{Jc(10)} - 20) \left(\frac{B_{10}}{B_{1T}} \right)^{1/4} \quad (3)$$

These data are replotted in **Figure 8** represented by rhombi. A set of twelve PCVN specimens was used, from which only two had valid K_{Jc} values and were only size corrected. The others were constraint adjusted and size corrected. Additionally, the reference temperature T_0 was established. The reference temperature T_0 was estimated to be -78.2°C , which is in good agreement with the value of $T_0 = -82^\circ\text{C}$ obtained by means of 1T specimens.

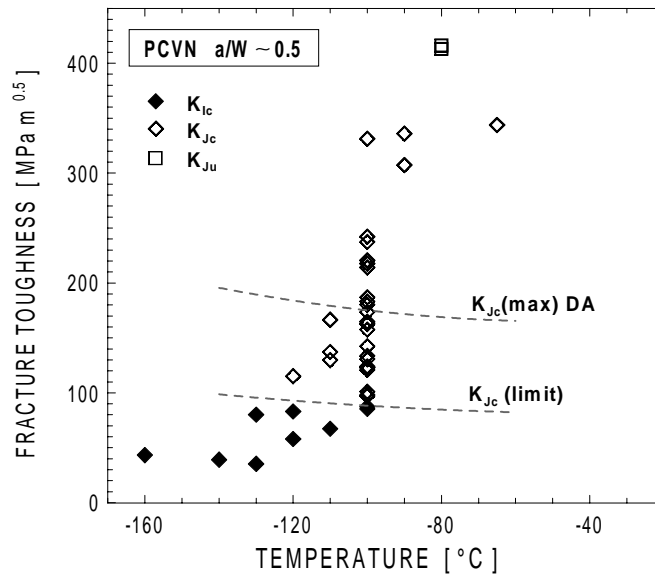


Figure 7: Fracture toughness determined using pre-cracked Charpy type specimens

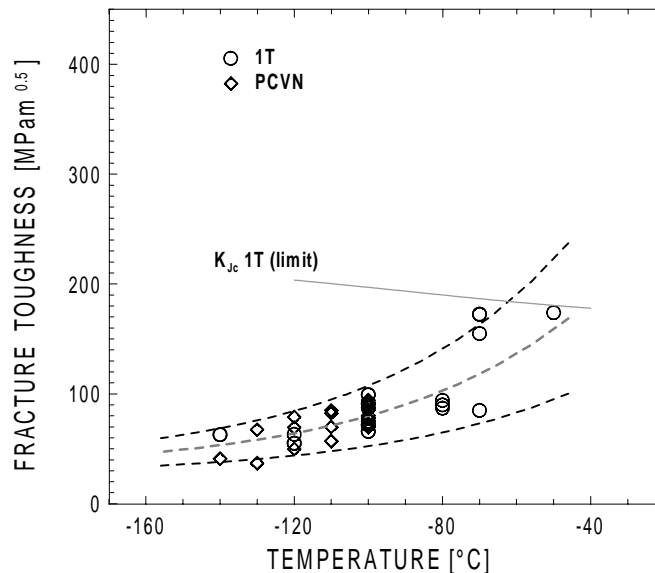


Figure 8: Predictions of 1T specimen behaviour using the PCVN specimen

The master curve $K_{Jc(med)}$ and tolerance bounds for 5 and 95% are plotted using the data obtained from the PCVN specimens in Figure 8. All fracture toughness data of the 1T specimens (round points) fall inside the scatter band of PCVN specimen assessed by the above-mentioned procedure, thus verifying the potential of utilising small pre-cracked specimens for the fracture toughness evaluation in the transition region.

CONCLUDING REMARKS

In the presented investigation the fracture resistance of ferritic steel intended for casks for spent nuclear fuels has been analysed combining several approaches.

The characteristics of crack length effect (and corresponding crack tip constraint effect) have been summarised for the steel investigated. The most important finding is the increase in cleavage fracture stress with decreasing crack length of bend specimens having the same ligament.

The toughness scaling model of Dodds and Anderson has been tested when transferring the fracture mechanical characteristics from the small Charpy type specimens on the 1T bend specimens.

A modified approach has been developed for Q-parameter determination taking into account large scatter of inherent material toughness and plastic deformation preceding the fracture. For these purposes the J-integral has been found to give more consistent data than standard calculation based on critical loads.

The master curve concept has been shown to be valid in the lower shelf and transition range for C-Mn cast steel. Reference temperature T_0 determined using constraint adjusted and size corrected PCVN data was only slightly different from T_0 evaluated using 1T SENB specimens.

ACKNOWLEDGEMENTS

The research was financially supported by the grant No. 101/96/K264 of the Grant Agency of the Czech Republic and the project No. 972655 supported in the frame NATO Science for Peace program.

REFERENCES

1. *Guidelines for safe design of shipping packages against brittle fracture*, IAEA-TECDOC-717 (1993).
2. Warnke, E.P., Bounin, D., (1997) Fracture Mechanics considerations concerning the revised IAEA-TECDOC-717 guidelines, *Transaction of 14th Int. Conf. On Structural Mechanics in Reactor Technology*, GMW/6, pp. 571-578.
3. Moulin, D., Yuritzin, T., Sert, G., (1995) An Overview of R&D Work Performed in France Concerning the Risk of Brittle Fracture of Transport Cask, *RAMTRANS*, Vol. 6, No. 2/3, pp. 145-248.
4. Beremin F.M., (1983) *Metal. Trans. A*, Vol. 14A, pp. 2277-2287.
5. Wiesner, C.S., Andrews, R.M., 1997, *A review of Micromechanical failure models for cleavage and ductile fracture*, TWI, rpt. 592/1997.
6. Kozák, V., Novák, A., (2000) Local Parameters Susceptibility Checkup using Fracture Toughness Data, contribution in Proceedings of this conference.
7. Ruggieri, C., Dodds, R.H., Wallin, K., (1998) *Eng. Fract. Mech.* Vol. 60, pp. 14-36.
8. Koppenhoefer, K.C., Dodds, R. H., (1997) *Eng. Fracture Mech.*, Vol 58, pp. 224 – 270.
9. *Standard Test Method For the Determination of Reference Temperature T_0 for Ferritic Steels in the Transition range*, ASTM, E1921-97.
10. Wallin, K., (1997) *In Advances in Fracture Research, ICF 9*, Eds. B. L. KariHaloo, Y. W. Mai, M.I. Ritchie, Pergamon, Amsterdam, pp. 2333-2344.
11. Chlup, Z., Holzmann, M., Dlouhý, I., (1999) Micromechanical Aspects and Methods of Constraint Effect Assessment, *Proc. of Conf. Engineering Mechanics*, Svratka, pp. 315-320.
12. McCabe, D. E., Sokolov, M. A., Nansland, R. K., (1997) *In Struct. Mechanics in Reactor Technology, 14 Int. Conference*, Vol. 4, division G, Lyon, France, , pp. 349-356.
13. Kozák, K., Holzmann, M., Dlouhý, I. (1997) *Trans of 14th Int. Conf. On Structural Mechanics in Reactor Technology*, pp. 681-688.
14. Dodds, R.H., Anderson, T.L., (1991) *Journal of Testing and Eval.* 19 pp.123-134.
15. Anderson, T.H., Dodds, R.H., (1991) *Inter J. Fracture* 48 pp 1-22.
16. Chlup, Z.,(2000) *Micromechanical Aspects of constraint Effect*, PhD theses, IPM AS CR